Author Manuscript

Author Manuscript

Author Manuscript

Author Manuscript

HHS Public Access

Author manuscript

Nat Neurosci. Author manuscript; available in PMC 2012 January 01.

Published in final edited form as:

Nat Neurosci. ; 14(7): 824–826. doi:10.1038/nn.2828.

Synaptic vesicle retrieval time is a cell-wide not an individual synapse property

Moritz Armbruster[1,2] and **Timothy A. Ryan**[2,*]

[1]David Rockefeller Graduate Program of Rockefeller University, 1230 York Avenue, New York, NY 10065

[2]The Department of Biochemistry, Weill Cornell Medical College, 1300 York Avenue, New York, NY 10065

Although individual nerve terminals from the same neuron often differ in neurotransmitter release characteristics the extent to which endocytic retrieval of synaptic vesicle components differs is unknown. We used high-fidelity optical recordings to undertake a large-scale analysis of endocytosis kinetics of individual boutons. Our data indicate that endocytosis kinetics do not differ substantially across boutons from the same cell but instead appear to be controlled at a cell-wide level.

Synaptic vesicle (SV) recycling ensures sufficient vesicles for ongoing synaptic function. Recent experiments demonstrated that SVs recycle locally in a clathrin[1], AP-2[2] and dynamin-dependent[3–5] manner. pHluorin-tagged SV proteins provides a powerful approach to monitor endocytosis kinetics in response to AP firing at the single synapse and single vesicle level[6]. We recently demonstrated that single vesicle retrieval is stochastic displaying exponentially distributed retrieval times. Larger stimuli (up to 150 AP) also lead to similar single exponential fluorescence decays, agreeing with the stochastic model's prediction for the many vesicle case and indicating that vesicles endocytose in parallel under these conditions. We sought to determine to what extent endocytosis kinetics are dictated at the single synapse versus cellular level. Our data reveal large variations in SV endocytosis time constants (τ_{endo}) between cells ranging from a mean of 5.5 s to 38.9 s that is independent of the history of chronic activity. Most variation between boutons of the same cell is explained by the expected stochastic endocytosis behavior of individual vesicles. Endocytosis retrieval times appear to be under the influence of a cell-wide modulator of endocytosis rather than set at the single synapse level.

Our observation that endocytosis of individual SVs is governed by a stochastic process predicts that one requires repeated sampling of endocytosis in order to properly characterize its kinetics at individual synapses. pHluorin-tagged vGlut1 (vG-pH) or Synaptophysin

Users may view, print, copy, download and text and data- mine the content in such documents, for the purposes of academic research, subject always to the full Conditions of use: http://www.nature.com/authors/editorial_policies/license.html#terms

*Corresponding Author: Timothy A. Ryan, Department of Biochemistry, Weill Cornell Medical College, 1300 York Ave, NY, NY 10065, taryan@med.cornell.edu.

Author Contributions:

M.A. and T.A.R. designed research; M.A. performed research; M.A. and T.A.R. analyzed data; and M.A. and T.A.R. wrote the paper.

Author Manuscript Author Manuscript Author Manuscript Author Manuscript

(physin-pH) expressed in individual dissociated hippocampal neurons provides a readout of endocytosis kinetics following exocytosis. The low-photobleaching rate and high sensitivity of pHluorin-based assays allowed us to interrogate endocytic performance repeatedly over many trials simultaneously at numerous nerve terminals. An individual experiment yielded between 12 and 131 boutons for analysis from which single bouton endocytosis kinetics could be measured (Fig 1A). We chose a 100 AP 10Hz stimulus to provide sufficient signal to noise allowing fitting of single trials to determine τ_{endo} (see below). This stimulus results in exocytosis of 24 ± 4% (n=8 cells) of the recycling pool, below the endocytic capacity of ~40%[7] of these neurons. τ_{endo} from pHluorin responses was measured over ~25–35 sequential stimulus runs for each neuron. Only experiments yielding stable response amplitude and kinetics across the experiment were used for analysis (Fig S1). Each fluorescence trace reveals the stimulus-locked exocytosis response (fluorescence increase) followed by a post-stimulus fluorescence decay which is the convolution of endocytic and reacidification dynamics. The curves were fit to single exponential decays (Fig 1B) beginning at a time point offset from the end of the stimulus equal to roughly twice the reacidification time constant where the exponential time course is dominated by endocytosis[6]. The robustness of the data set was maximized by imposing stringent criteria for inclusion of individual events based on fit quality, temporal stability and signal to noise (see Methods). In total our initial analysis included 23,738 individual trial responses from a total of 1793 boutons associated with 49 neurons.

Data associated with an individual cell is represented as a heat map, color coded to show τ_{endo} values obtained for the 300–1200 events measured across all boutons of an individual cell (Fig 1C). The mean τ_{endo} for each bouton in turn allowed us to determine the variance of τ_{endo} across boutons within a given cell. For the example shown in Figure 1D, the coefficient of variation CV) across boutons was ~19%, similar to the mean intrabouton CV determined from many cells (17.5 ± 0.9% N=34 cells). Contributions to the CV are expected to arise from at least two sources: (1) for each bouton, endocytosis is likely stochastic, and therefore will lead to inherent variations that can only be averaged out with sufficient measurement repetition; (2) the characteristic τ_{endo} for each bouton may be genuinely different (a biological variation). In order to determine the relative contributions of these to the CV, we took two approaches. We first used a “boot-strap” approach, whereby one tests the hypothesis that fluctuations arise non-randomly by recalculating the average CV after many random reshuffles of the data[8]. Variations across boutons due to insufficient sampling would result in a distribution of CVs obtained after reshuffling the data covering the original data set. Averaged across 500 permutations per cell the boot-strap approach predicts a CV of 9.4 ± 2.5% (standard deviation) indicating that a large portion of the experimental average CV (17.5 ± 0.9%) likely arises from too limited a sampling of a stochastic process. We also explicitly calculated, from a theoretical standpoint, the degree of fluctuation expected based upon the single vesicle description of endocytosis as an exponentially distributed stochastic process[6]. The model was extended to a several vesicle Markov Model where each of *n* vesicles are internalized independently with the same stochastic parameter (see Methods). The distribution of all bouton events from individual cells was then fit to the Markov model with only two free parameters, *n* and $<\tau_{endo}>$(Fig 1E). The data shows that individual τ_{endo} span a wide range, from ~3s to 40s. These extremes in the distribution are expected from a

Author Manuscript Author Manuscript Author Manuscript Author Manuscript

stochastic process, as is verified by the fact that the entire distribution is accurately fit by the *n*-vesicle Markov model. The model's prediction of the number of vesicles internalized, 17 ± 1 (N=34 cells), compares well to our experimental estimate of 15 ± 2 for this stimulus (see Methods). The model also allows one to estimate the expected coefficient of variation across boutons assuming they have identical properties incorporating the measured fluctuations in exocytosis. The Markov model predicts that for a similar data set the coefficient of variation between identical boutons would be ~12% (Methods). Thus both the bootstrap and the explicit theoretical approach agree very well and indicate that a large fraction of the measured CV in τ_{endo} across boutons is expected from the stochastic nature of endocytosis.

Given that a given cell's distribution of τ_{endo} values is well described by the Markov model, we conclude that the parameter $<\tau_{endo}>$is a good descriptor of endocytic behavior of that cell. Unlike the case for individual boutons, the estimate of cell average $<\tau_{endo}>$ is based on hundreds (300–1200) of individual bouton-events. This analysis allowed us to compare $<\tau_{endo}>$ values across many cells. Given that our data indicate that endocytosis is well characterized by a cell-wide property, we reasoned that one could obtain valid estimates from of $<\tau_{endo}>$ using fewer repetitions (50–250 bouton events) allowing us to increase the total sample size for this aspect of the analysis. Following this reasoning we expanded the data set to a total of 84 individual cells. These data showed that unlike for individual boutons, individual cells showed a large degree of variation in $<\tau_{endo}>$. Over the entire distribution of cells (N=84) the cell $<\tau_{endo}>$ ranged from 5.5s to 38.9s with a CV of 41% (Fig 2B). These data indicate that each cell has its own endocytic kinetics, and that these kinetics differ significantly across cells.

We wondered if $<\tau_{endo}>$ might be correlated with neurotransmitter type, age in culture or history of chronic activity. Age in culture showed no significant trend in $<\tau_{endo}>$ over the 8 day range of ages used (Fig S2). We used retrospective vGlut and/or vGat immunocytochemistry to determine if variation in endocytosis kinetics might be correlated with the type of neurotransmitter being release (Fig S3). These experiments revealed that both groups showed a wide range of $<\tau_{endo}>$ with no statistically significant difference between the distributions (Fig 2C). Individual neurons appear to adjust key properties associated with synaptic transmission in response to levels of chronic activity, known as a homeostatic scaling. Given the cell-wide but cell-specific character of endocytosis kinetics we sought to determine if this presynaptic parameter was under homeostatic feedback control. To test this idea τ_{endo} measurements were obtained from neurons in which electrical activity had been chronically silenced for 2–8 days using TTX. We recently showed that such treatments result in acceleration in exocytosis kinetics and increases in the size of the synaptic vesicle recycling pool[9], however these experiments showed that the endocytic profile of cells appears invariant with respect to the history of chronic activity, irrespective of neurotransmitter type (Fig 2C).

Finally we examined whether variability in $<\tau_{endo}>$ would be sensitive to perturbations known to dramatically slow endocytosis. We made use of shRNA-mediated knockdown of the clathrin adaptor AP-2 (Fig S4), resulting in 3-fold slowing of SV endocytosis[2] (Fig 2C,S6), consistent with the observations that SV endocytosis is largely a clathrin-mediated process. As with WT neurons, we found significant variability in $<\tau_{endo}>$ from cell to cell

Author Manuscript Author Manuscript Author Manuscript Author Manuscript

(WT $CV_{<\tau endo>}$ = 41% (95% confidence interval 34%–49%), AP-2 KD $CV_{<\tau endo>}$= 56% (95% confidence interval 24%–82%)[10]) (Fig. 2C) that was unrelated to the degree of knockdown (Fig S5). Thus the mechanism of the cell to cell variations in endocytosis remains intact despite dramatic slowing of the endocytic process.

The molecular mechanisms and kinetics of SV endocytosis have been of significant interest since the discovery of SV recycling [11]. Although the importance of a clathrin-mediated pathway in SV endocytosis has been established it is unknown what feature of this pathway controls speed. Use of pHluorin reporters allowed for acquisition of large data sets from individual cells, enabling us to examine fluctuations in τ_{endo} for the first time. The most parsimonious explanation of the observed fluctuations in τ_{endo} within a given cell is that they arise from the stochastic nature of endocytosis itself. The agreement between the observed distribution in τ_{endo} and a Markov model of the expected number of vesicles endocytosing (Fig 1E) suggests that most fluctuations within a given cell can be accounted for from the sampling statistics. This places an upper bound on the amount of biological variation between boutons. Assuming that in addition to sampling errors the CV is also impacted by variations in exocytosis, the upper bound for the expected CV across boutons is ~12% (see Supp. Model). In contrast our analysis of $<\tau_{endo}>$ across 84 cells indicates that there is almost 4-fold greater variability in this parameter across cells. Thus endocytic performance is a cell-wide parameter. Given that exocytosis properties have been shown to vary significantly across synapses[12], these results suggest that endocytosis is largely uncoupled from aspects of exocytosis. Consistent with these findings we found that chronic silencing of neurons, previously shown to lead to up regulation of both pre[13] and postsynaptic[14] aspects of synaptic transmission, did not lead to measurable changes in the $<\tau_{endo}>$. Our data indicate that the key parameter describing endocytic performance is set at the single cell level, perhaps reflecting a regulatory program related to specific, but as yet unidentified elements of the endocytic machinery. The fact that perturbations of a protein that participates in endocytosis (AP-2) dramatically slows endocytosis but leaves the variability intact suggests the existence of a cell-wide modulatory system that influences SV retrieval time. The identity of this modulatory system remains unknown however its existence predicts a potentially powerful means of controlling presynaptic performance.

Supplementary Material

Refer to Web version on PubMed Central for supplementary material.

Acknowledgments

The authors would like to thank members of the Ryan lab and Jeremy Dittman for useful discussions and Ricky Kwan for excellent technical assistance. vGlut-pHluorin was kindly provided by Susan Vogelmeier and Robert Edwards and the synaptophysin-pHluorin construct was kindly provided by Yongling Zhu (Salk Institute). This work was supported by grants from the NIH (TAR) as well as the David Rockefeller Graduate School of the Rockefeller University.

References

1. Granseth B, Odermatt B, Royle SJ, Lagnado L. Neuron. 2006; 51:773–786. [PubMed: 16982422]
2. Kim SH, Ryan TA. J Neurosci. 2009; 29:3865–3874. [PubMed: 19321783]

Author Manuscript Author Manuscript Author Manuscript Author Manuscript

3. Koenig JH, Ikeda K. J Neurobiol. 1983; 14:411–419. [PubMed: 6139412]
4. Newton AJ, Kirchhausen T, Murthy VN. PNAS. 2006; 103:17955–17960. [PubMed: 17093049]
5. Ferguson SM, et al. Science. 2007; 316:570–574. [PubMed: 17463283]
6. Balaji J, Ryan TA. Proc Natl Acad Sci U S A. 2007; 104:20576–20581. [PubMed: 18077369]
7. Balaji J, Armbruster M, Ryan TA. J Neurosci. 2008; 28:6742–6749. [PubMed: 18579748]
8. Elston, RCaJ; William, D. Basic biostatistics for geneticists and epidemiologists: a practical approach. Chichester, U.K.: John Wiley & Sons; 2008.
9. Kim SH, Ryan TA. Neuron. 2010; 67:797–809. [PubMed: 20826311]
10. Vangel MG. The American Statistician. 1996; 15:21–26.
11. Heuser JE, Reese TS. J Cell Biol. 1973; 57:315–344. [PubMed: 4348786]
12. Branco T, Staras K, Darcy K, Goda Y. Neuron. 2008; 59:475–485. [PubMed: 18701072]
13. Murthy VN, Schikorski T, Stevens CF, Zhu Y. Neuron. 2001; 32:673–682. [PubMed: 11719207]
14. Turrigiano GG. Cell. 2008; 135:422–435. [PubMed: 18984155]
15. Ryan TA. J Neurosci. 1999; 19:1317–1323. [PubMed: 9952409]

Author Manuscript Author Manuscript Author Manuscript Author Manuscript

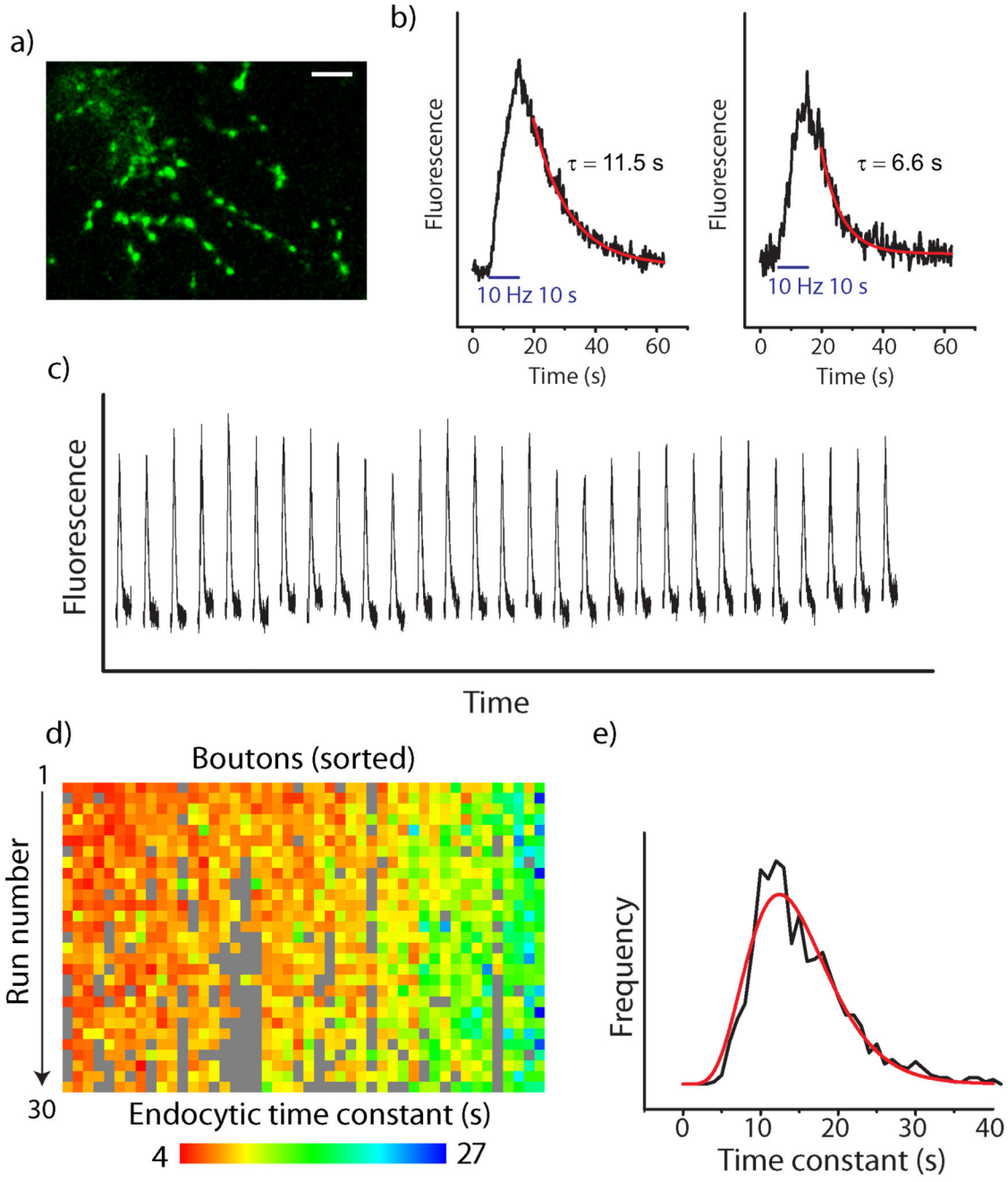

Figure 1.

A) Representative field of synaptic boutons transfected with vG-pH. Scale bar 10μm. B) example traces with exponential fits to the fluorescence decays of a single bouton stimulated with 100AP 10Hz stimulus. Decay times are 11.5 ±0.5 s and 6.6 ±0.4 s respectively. C) exo-endocytic responses from 29 consecutive runs from a single bouton with 5 min recovery between runs. D) Heat map of all endocytic decays of an individual cell, color-coded from 4s (red) to 27s (blue), with grey being events that did not pass inclusion criteria. Boutons are sorted from fastest (left) to slowest (right); while runs are from first (top) to last (bottom).

Author Manuscript Author Manuscript Author Manuscript Author Manuscript

(29 runs, 46 boutons, 1136 events, average time constant 9.2s ± 0.1s). E) Histogram of all 832 bouton events from a single cell plotted with the maximum-likelihood fit of the Markov model (Histogram (black) mean $<\tau_{endo}>$= 14.50 s, Model (red) mean $<\tau_{endo}>$= 15.22 s, N=19 vesicles).

Author Manuscript Author Manuscript Author Manuscript Author Manuscript

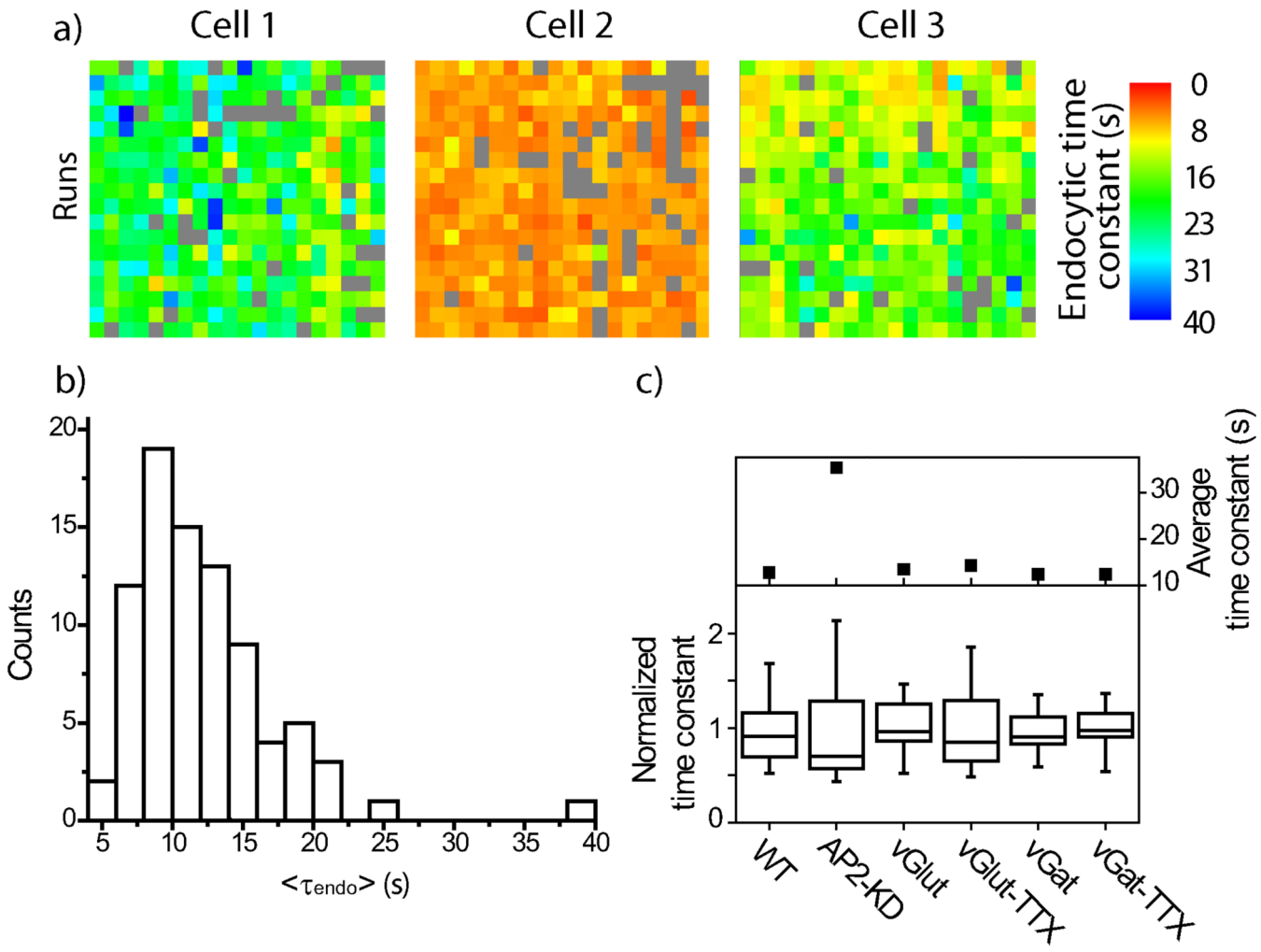

Figure 2.

A) Heat maps of 3 different cells (truncated to 18 runs (top to bottom) and 20 boutons each). Grey represents bouton-events that did not meet inclusion criteria. (Average τ_{endo} 20.7±0.3s, 6.3±0.1s, 15.7±0.3s) B) $<\tau_{endo}>$ distribution across cells shows a range from 5.5s – 39.8s (N=84 cells) C) Distribution and $<\tau_{endo}>$ of WT, AP2-KD, vGlut-positive, vGlut-positive TTX silenced, vGat-positive and vGat-positive TTX silenced cells based upon post-experiment immunofluorescence staining. Normalizing the distributions to their mean showed that there is no significant difference in the spread of the distribution for AP2-KD cells compared to WT (KS-test p=0.29). Silencing cultures with TTX for 2–8 days showed no significant difference in their distributions (KS-test p=0.24 vGlut, p=0.69 vGat). vGlut, vGat segregation showed no significant difference in their distributions (KS-test p=0.28). (Box-whisker plots showing 5%–25%–50%– 75%–95%) is plotted. (WT N= 84, AP2-KD N=14, vGlut N=10, vGlut-TTX N=14, vGat N=16, vGat-TTX N=11 cells) Cell averaged time constants WT 12.3±0.6s, AP2-KD 35.3±5.3s, vGlut 13.4±0.8s, vGlut-TTX 14.3±1.5s, vGat 13.4±0.9s, and vGat-TTX 12.4±0.9s.